

Subband structure of a nearly free, uniform-density, dilute electron system in a wide quantum well

T. Sajoto, J. Jo, L. Engel, M. Santos, and M. Shayegan

Department of Electrical Engineering, Princeton University, Princeton, New Jersey 08544

(Received 13 January 1989)

Quantum oscillations in the magnetoresistance of an electron system realized in a selectively doped, wide parabolic quantum well of $\text{Al}_x\text{Ga}_{1-x}\text{As}$ are analyzed to obtain the electron densities of the electric subbands. Self-consistent calculations of the subband structure predict that the electrons in the well occupy four electric subbands, and that the total electron wave function is nearly constant over the central 1000 Å of the well. The measured subband densities agree with the predictions of the calculation remarkably well, verifying the realization of the electron system designed.

In selectively doped semiconductor structures, the carriers are spatially separated from the dopant atoms to reduce the ionized-impurity scattering. Because of the reduced disorder and scattering, these structures provide a nearly ideal system for the study of many-body effects. The high-mobility two-dimensional electron system at the interface of $\text{GaAs}/\text{Al}_x\text{Ga}_{1-x}\text{As}$, for example, made the discovery of the fractional quantum Hall effect possible and has been used to observe new quantum phenomena.¹ Studies of the electron-electron interaction effects can be extended to three-dimensional (3D) semiconductor systems. In fact, a variety of collective phenomena such as charge-density waves, spin-density waves, and Wigner crystallization have been theoretically proposed to occur in dilute 3D free-electron systems under appropriate conditions (e.g., at very low temperatures and in intense applied magnetic fields).² Experimentally, dilute electron systems in uniformly doped degenerate semiconductors have been studied extensively; however, the electron-impurity interaction in these systems is strong and usually leads to the magnetic freeze-out of the carriers. Realization of a 3D dilute electron system with low disorder is, therefore, of considerable interest.

We recently reported the fabrication of a selectively-doped semiconductor structure which may be considered as a first step towards the realization of a 3D or quasi-3D free-electron system.^{3,4} Such structures were suggested in Ref. 2 and were recently grown using molecular-beam epitaxy by Shayegan and co-workers^{3,4} and independently by Sundaram *et al.*⁵ Magnetotransport^{3,4} and magneto-optical⁶ measurements on our structures revealed that the system contains $\sim 2.5 \times 10^{11} \text{ cm}^{-2}$ electrons, which occupy four electric subbands and have a low-temperature mobility of $\sim 1.2 \times 10^5 \text{ cm}^2/\text{Vs}$, indicating the high quality of the structure.³ Magnetotransport data on similar structures have also been reported by Gwinn *et al.*⁷ These measurements, however, do not provide quantitative information on the subband structure of these systems. In this Rapid Communication, we report low-temperature ($T \approx 30 \text{ mK}$) magnetotransport measurements from which we obtain the subband densities in our structure. The excellent agreement of these measured densities with the results of our self-consistent calculations of the sub-

bands provides clear, quantitative evidence for the realization of the electron system designed.

The details of our structure (M77) and its growth parameters were given previously.^{3,4} It consists of a 2000-Å-wide undoped $\text{Al}_x\text{Ga}_{1-x}\text{As}$ well bounded by undoped (spacer) and doped layers of $\text{Al}_y\text{Ga}_{1-y}\text{As}$ ($y > x$) on two sides. The alloy composition (x) in the well is graded quadratically, from $x=0$ at the center of the well to $x=0.19$ at the edges of the well, while the Al composition in the barrier is $y=0.27$.³ In the absence of any space charge, and assuming that the conduction-band offset for $\text{GaAs}/\text{Al}_x\text{Ga}_{1-x}\text{As}$ is linearly proportional to x , this compositional grading in the well is expected to result in a parabolic potential well as shown in Fig. 1 (curve *a*). Classi-

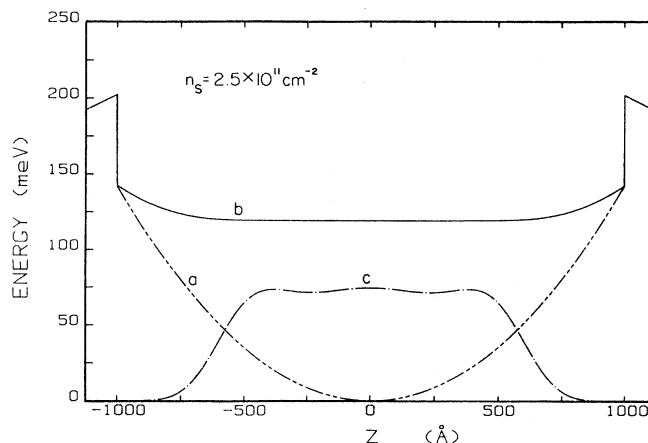


FIG. 1. The conduction-band edge of the structure in the absence of any space charge is shown by curve *a*. We assumed that the conduction-band offset for $\text{GaAs}/\text{Al}_x\text{Ga}_{1-x}\text{As}$ heterostructure is equal to $750x$ (in units of meV) (Ref. 8). Curve *b* shows the self-consistently calculated potential for $n_s = 2.5 \times 10^{11} \text{ cm}^{-2}$. The total electron wave function, calculated by appropriately summing the wave functions of the four occupied subbands is shown by curve *c* (with an arbitrary scale). The energies of the occupied subbands, with respect to the bottom of the final conduction band (curve *b*), are $E_0=0.30 \text{ meV}$, $E_1=1.09 \text{ meV}$, $E_2=2.26 \text{ meV}$, and $E_3=3.75 \text{ meV}$; and the Fermi level $E_F=4.08 \text{ meV}$. The subband densities are given in Table I.

TABLE I. The calculated and measured subband densities for the structure we studied are listed as percentages of the total density n_s . The calculation assumes a total electron density $n_s = 2.5 \times 10^{11} \text{ cm}^{-2}$, and the total measured density (determined from the positions of the ρ_{xx} minima at low filling factors) is $2.45 \times 10^{11} \text{ cm}^{-2}$.

	Subband densities (as percentages of n_s)			
	n_0	n_1	n_2	n_3
Calculated	42.4	33.5	20.4	3.7
Measured	43.3	32.7	20.8	3.2

cally, once the electrons are transferred into this well, they screen the parabolic potential and a system of nearly uniformly distributed electrons in a flat potential can be expected.³⁻⁷

Quantum mechanically, the finite width of the well leads to the quantization of the energy levels. In the Hartree approximation (neglecting exchange correlation), the subband structure of the system can be determined by solving the Poisson and Schrödinger equations self-consistently. We performed such calculations to find the energy levels and the eigenfunctions for this structure. The final, self-consistent potential and the total electron wave function are shown in Fig. 1 as curves *b* and *c*, respectively. This calculation indicates that for the measured electron areal density in our structure ($n_s \sim 2.5 \times 10^{11} \text{ cm}^{-2}$), four electric subbands are occupied. The calculated subband densities are given in Table I. Despite the relatively small number of occupied subbands, the electron density is fairly constant over a wide distance ($\sim 1000 \text{ \AA}$). If the effective width of the wave function is taken to be $\approx 1000 \text{ \AA}$, then the 3D electron density in the well is $\sim 2.5 \times 10^{16} \text{ cm}^{-3}$.⁹

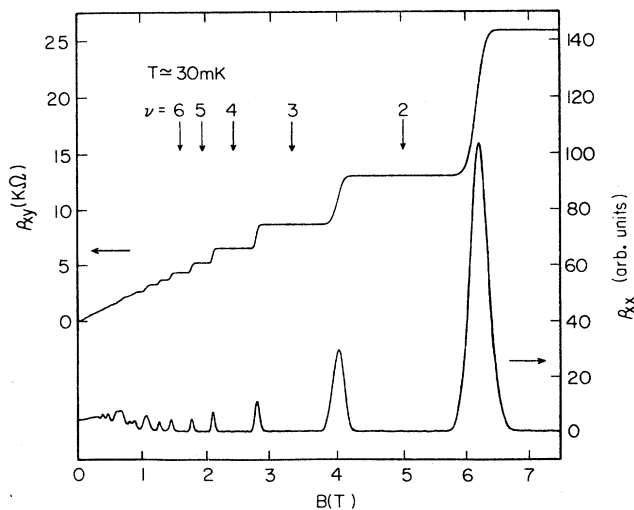


FIG. 2. Magnetotransport coefficients ρ_{xx} and ρ_{xy} for sample *M77* are shown for $T \sim 30 \text{ mK}$. The vertical arrows indicate the Landau-level filling factors (ν) at which the integral quantum Hall effect is observed.

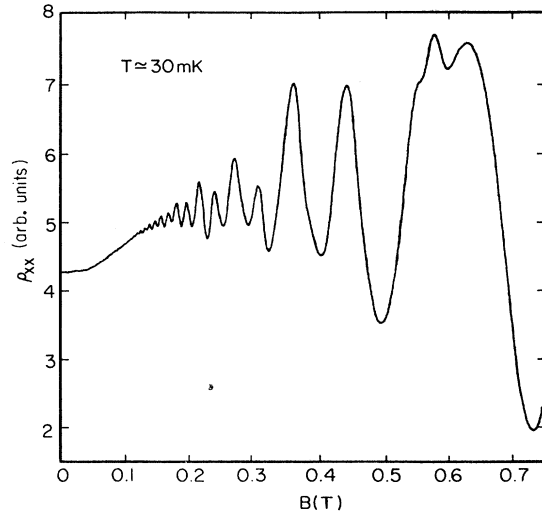


FIG. 3. The ρ_{xx} data for sample *M77* are shown in detail at low magnetic field.

In order to characterize this system and to determine the subband structure, we measured the magnetotransport coefficients at milliKelvin temperatures in the Hall bridge geometry. Contacts were made by alloying In in a hydrogen atmosphere at 400°C for 3–5 min. We measured the transverse (ρ_{xx}) and Hall (ρ_{xy}) resistivities in the conventional manner (magnetic field \mathbf{B} in the z direction perpendicular to the plane of the sample), as well as the longitudinal resistivity (ρ_{zz}) with \mathbf{B} in the plane of the sample along the direction of the current.

The ρ_{zz} data exhibit quantum oscillations as a function of magnetic field.³ These oscillations are associated with the depopulation of the hybrid (electric-magnetic) subbands as \mathbf{B} increases, and indicate that four electric subbands are occupied at $\mathbf{B} = 0$.³ This observation is in qualitative agreement with the subband structure shown in Fig.

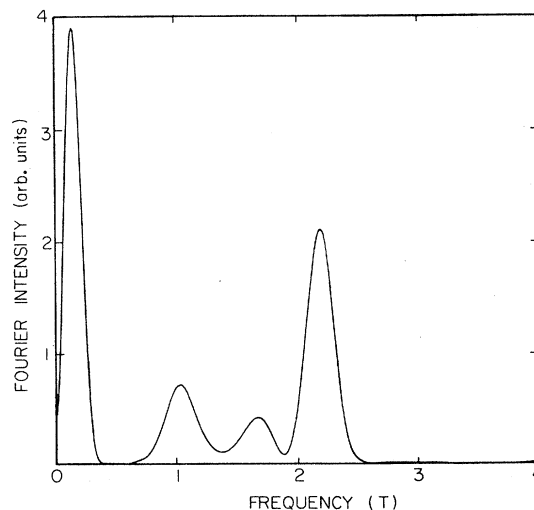


FIG. 4. The FFT power spectrum of the oscillatory ρ_{xx} data vs $1/B$ in the low-field range ($B < 0.75 \text{ T}$) is shown.

1. The low-temperature ρ_{xx} and ρ_{xy} data shown in Figs. 2 and 3, on the other hand, can be used to obtain *quantitative* information about the subband structure. The data in Fig. 2 were measured at $T \sim 30$ mK, and exhibit quantum Hall effect. The vertical arrows in Fig. 2 indicate the Landau-level filling factors (ν) at which the integral quantum Hall effect is observed. The positions (in magnetic field) of ρ_{xx} minima and ρ_{xy} plateaus for $B \gtrsim 1$ T are consistent with an areal density $n_s = (2.45 \pm 0.05) \times 10^{11} \text{ cm}^{-2}$. It is interesting to note that in the field range of $B \gtrsim 2$ T, the Landau-level versus B fan diagram indicates that only the $N=0$ Landau levels of the lowest electric subbands are occupied.

In the low-field range, many Landau levels of each subband are occupied. The oscillatory magnetoresistance data in this range are periodic in $1/B$ and contain several oscillation frequencies (Fig. 3). These frequencies, which are directly proportional to the areas of the Fermi surface cross sections,¹⁰ can be found from the fast Fourier transform (FFT) of the ρ_{xx} vs $1/B$ data.¹¹ The FFT power spectrum of the ρ_{xx} data of Fig. 3 is shown in Fig. 4. The positions of the peaks in the FFT power spectrum give the areas of the Fermi-surface cross sections (circles in our case), and therefore the electron densities for the different occupied electric subbands (n_i for $i=0,1,\dots$). These measured densities are $n_0=1.06$, $n_1=0.80$, $n_2=0.51$, and

$n_3=0.08$ in units of 10^{11} cm^{-2} , and are listed in Table I.¹² The excellent agreement between the measured and calculated densities for each subband is quite remarkable.

In summary, we have reported magnetotransport data and self-consistent calculations that provide clear and quantitative evidence for the realization of a low-disorder (high-mobility), dilute, quasi-three-dimensional electron system with a nearly uniform density over a wide distance of $\sim 1000 \text{ \AA}$. We plan to grow similar low-disorder structures with wider wells and more uniform total electron wave functions; such structures are expected to better approximate a 3D free-electron system.

Note added in proof. Inclusion of the exchange-correlation effects in the local-density-functional approximation¹³ changes the calculated subband densities very slightly. We find 42.8, 34.2, 20.6, and 2.4 for the subband densities n_0 , n_1 , n_2 , and n_3 , respectively (expressed as percentages of $n_s = 2.5 \times 10^{11} \text{ cm}^{-2}$; cf. Table I).

We thank D. C. Tsui for useful discussions. Support of this work by the National Science Foundation Grants No. DMR-8705002, No. DMR-8212167, and No. ECS-8553110; Grant No. DAAG9-85-K-0098 by the Army Research Office; and grants by the General Telephone and Electronics Laboratories, Inc., and the New Jersey Commission on Science and Technology are acknowledged.

¹For a review, see D. C. Tsui and H. L. Störmer, *IEEE J. Quantum Electron.* **QE-22**, 1711 (1986).

²B. I. Halperin, *Jpn. J. Appl. Phys.* **26**, Suppl. 26-3, 1913 (1987).

³M. Shayegan, T. Sajoto, M. Santos, and C. Silvestre, *Appl. Phys. Lett.* **53**, 791 (1988).

⁴T. Sajoto, J. Jo, H. P. Wei, M. Santos, and M. Shayegan, *J. Vac. Sci. Technol.* (to be published).

⁵M. Sundaram, A. C. Gossard, J. H. English, and R. M. Westervelt, *Superlattices Microstruct.* **4**, 683 (1988).

⁶K. Karrai, H. D. Drew, M. W. Lee, and M. Shayegan, *Phys. Rev. B* **39**, 1426 (1989); M. Shayegan, M. Santos, T. Sajoto, K. Karrai, M. W. Lee, and H. D. Drew, in *Magnetic Fields in Semiconductor Physics II*, edited by G. Landwehr (Springer-Verlag, Berlin, in press).

⁷E. G. Gwinn, R. M. Westervelt, P. F. Hopkins, A. J. Rimberg, M. Sundaram, and A. C. Gossard, *Superlattices Microstruct.* (to be published); E. G. Gwinn, P. F. Hopkins, A. J. Rimberg, and R. M. Westervelt, in *Magnetic Fields in Semiconductor Physics II*, edited by G. Landwehr (Springer-Verlag, Berlin, in press); E. G. Gwinn, R. M. Westervelt, P. F. Hopkins, A. J. Rimberg, M. Sundaram, and A. C. Gossard, *Phys. Rev. B* **39**, 6260 (1989).

⁸See, e.g., R. C. Miller, A. C. Gossard, D. A. Kleinman, and O. Munteanu, *Phys. Rev. B* **29**, 3740 (1984).

⁹It is worth noting that for a somewhat larger n_s , the width of the total electron wave function increases while the 3D electron density and the Fermi level of the system remain essentially unchanged (Ref. 4). This is the expected behavior for electrons in a parabolic well in the limit that many subbands are occupied.

¹⁰See, e.g., N. W. Ashcroft and N. D. Mermin, *Solid State Physics* (Holt, New York, 1976), p. 264.

¹¹We first subtracted a smooth (quadratic) background from the ρ_{xx} data of Fig. 3 in the range of $0.12 < B < 0.75$ T to obtain the oscillating part of ρ_{xx} . The FFT of this oscillatory ρ_{xx} vs $1/B$ was then calculated (Fig. 4).

¹²The accuracy for our measured n_0 , n_1 , and n_2 is $\approx \pm 2\%$. The position of the lowest frequency peak in the FFT spectrum of Fig. 4 is not accurate because it is affected substantially by the range of the B field over which the FFT spectrum is calculated. We determined n_3 by subtracting $n_0+n_1+n_2$ from $n_s = 2.45 \times 10^{11} \text{ cm}^{-2}$ (the density determined from the positions of ρ_{xx} minima in the range of $B > 1$ T).

¹³F. Stern and S. Das Sarma, *Phys. Rev. B* **30**, 840 (1984).